

## CHAPTER V

### EXPERIMENTS

The substrate preparation and the metal deposition are described in the section 5.1. There are two methods to deposit the metals, evaporation for Au and Ni, and sputtering for Mo. For Au/p-CuInSe<sub>2</sub> and Ni/p-CuInSe<sub>2</sub>, the DACCT measurement can be applied, the typical results are in the section 5.2.

For different workers using different techniques, it is hard to compare their experimental results. So, we report the total resistance, in the section 5.3. And also calculate the maximum contact resistivity, by not subtracting any resistance from the total resistance.

For the Mo/p-CuInSe<sub>2</sub>, the contact resistance is too high. Even the DACCT measurement can not be carried out because of the unsteadiness of the signal. A crude method in the section 5.4, I-V characteristic of two equal contacts on the same substrate's surface, is used. This measurement is merely served to indicate the order of magnitude of the contact resistivity and the poor nature of Mo/p-CuInSe<sub>2</sub> contact. Reproducible measurements were obtained however on Au/p-CuInSe<sub>2</sub> and Ni/p-CuInSe<sub>2</sub> (see discussion in the section 7.9).

The p-CuInSe<sub>2</sub> samples prepared by the available technique are not very homogeneous (see discussion in the section 7.8). This precluded the contact resistivity measurements which rely on homogeneous semiconductor and/or the

equal properties of each contact, for example, Cox and Strack (1967) method, and the two terminal contact resistance method (see Schroder, 1990). However, one is interested in measuring the value of the contact resistivity of the circular dot. Such measurement of the contact resistivity is described in the section 5.5. The configuration used is a modified form of Fahrenbruch and Bube (1983) technique which used three probes in their measurement. The value of the contact resistivity obtained by this measurement (see Table 4) indicates that the most of total resistance is due to the small contact (including the high resistive layer beneath the small contact).

### 5.1 Substrate Preparation and Metal Deposition

Different compositions of single crystal  $\text{CuInSe}_2$  were grown by the gradient freeze method. Normally in the same ingot only one type of conductivity, i.e. p or n type obtains. Typical substrate,  $4 \times 4 \times 1 \text{ mm}^3$ , were cut randomly from ingots, boiled in thinner for 5 min, acetone for 5 min, methanol for 5 min, then flushed with water, and then type-checked by the hot-probe method. By using evaporated Au as ohmic contact, the resistivity and carrier concentration were measured at room temperature in the van der Pauw configuration, except for the large substrate, i.e. #B4/11, on which ordinary (linear) configuration was used. The results were shown in Table 1 below.

TABLE 1

Resistivity and carrier concentration of substrates at room temperature.

#Substrate	Composition (0.3 at.%)	Resistivity ( $\Omega$ - cm)	Carrier Concentration ( $\times 10^{17}$ cm $^{-3}$ )
D3/1	deficient Cu	0.63	1.2
D3/3	" "	0.52	nd.
D3/4	" "	0.57	nd.
D3/5	" "	0.48	nd.
B4/9	stoichiometry	0.40	2.4
B4/11	" "	0.39	2.9
B4/12	" "	0.31	3.3
B4/17	" "	0.39	2.7
B4/18	" "	0.47	2.9
B3/5	excess Se	0.37	nd.
C3/15	" "	0.43	4.4
C3/16	" "	0.51	4.2
C3/19	" "	0.30	6.1
C3/20	" "	0.59	4.0
C3/25	" "	0.38	4.5
C3/26	" "	0.45	4.2
C3/27	" "	0.58	3.8
B6/1	excess Cu	0.45	2.9
B6/3	" "	0.34	3.2
B6/4	" "	0.53	2.4



The surface of each substrate was abrasively polished with 1 and 0.3  $\mu\text{m}$  alumina powder respectively, until a shiny surface is obtained. The best surface was chemically etched in fresh ( $\approx 25$  min after preparation)  $\text{HCl}:\text{HNO}_3:\text{H}_2\text{O}$ ; 13.5:7.5:5 (by volume) for 15 s, acetone for 15 s, methanol for 15 s, ultrasonic cleaning in deionised water, blown with dry nitrogen and subsequently transferred to a vacuum chamber. Stainless steel sheet having many pairs of circular holes, with a typical area of  $9.5 \times 10^{-3} \text{ cm}^2$  and centers about 2 mm apart, were used as masks.

For Au and Ni, in the vacuum chamber of about  $10^{-6}$  Torr of oil diffusion pump (no oil trap), the shutter was initially closed for 20 s, then Au or Ni was evaporated by molybdenum boat heater. The metal film of about 1500 angstroms thickness, measured by Edwards FTM5, was obtained. This metal film dot is referred as the small area metal contact which is the contact of interest. The other surface was evaporated in the same manner, using large hole mask. On this surface the area which did not get metal was sandblasted, and stuck onto the copper holder with silver paste. This surface was referred to as large area metal contact. The small area metal contact was electrically wired by means of a silver paste. The device was then exposed to a lamp to cure the silver paste.

For Mo/p-CuInSe<sub>2</sub> contacts, dc-sputtering was used. The pressure was first pumped to about  $1 \times 10^{-3}$  Torr, then Mo is sputtered at about  $30 \times 10^{-3}$  Torr. The sputtering deposition rate was about 150 angstroms /min .

## 5.2 Typical Results of DACCT Measurement

To accomplish the DACCT measurement, the device, such as in Fig.2, was first cooled by liquid nitrogen. While temperature relaxed to room temperature, the step constant currents which are described in Appendix B were applied, at 0.01 , 0.03, 0.1, 0.3, 1.03 and 4.95 mA, respectively. After the highest current was applied, the device was let stand without applied voltage for about 5 seconds. Then another voltage polarity was applied starting at the lowest current. The applied voltages for both polarities as a function of thermocouple voltage (type J), were recorded by a graph recorder. The example of the data on the graph is shown in Fig 6. Since the temperature-thermocouple voltage relationship is not strictly linear, reading the temperature values off from figure 6 is difficult. The x-axis scale is therefore converted to show data points vs. linear temperature scale. The typical patterns of Au/p-CuInSe<sub>2</sub> and Ni/p-CuInSe<sub>2</sub>, replotted at equal thermocouple voltage increments from graph paper, are now shown in Fig. 7 and 8, respectively with linear temperature x-axis.

ศูนย์วิทยทรัพยากร  
จุฬาลงกรณ์มหาวิทยาลัย

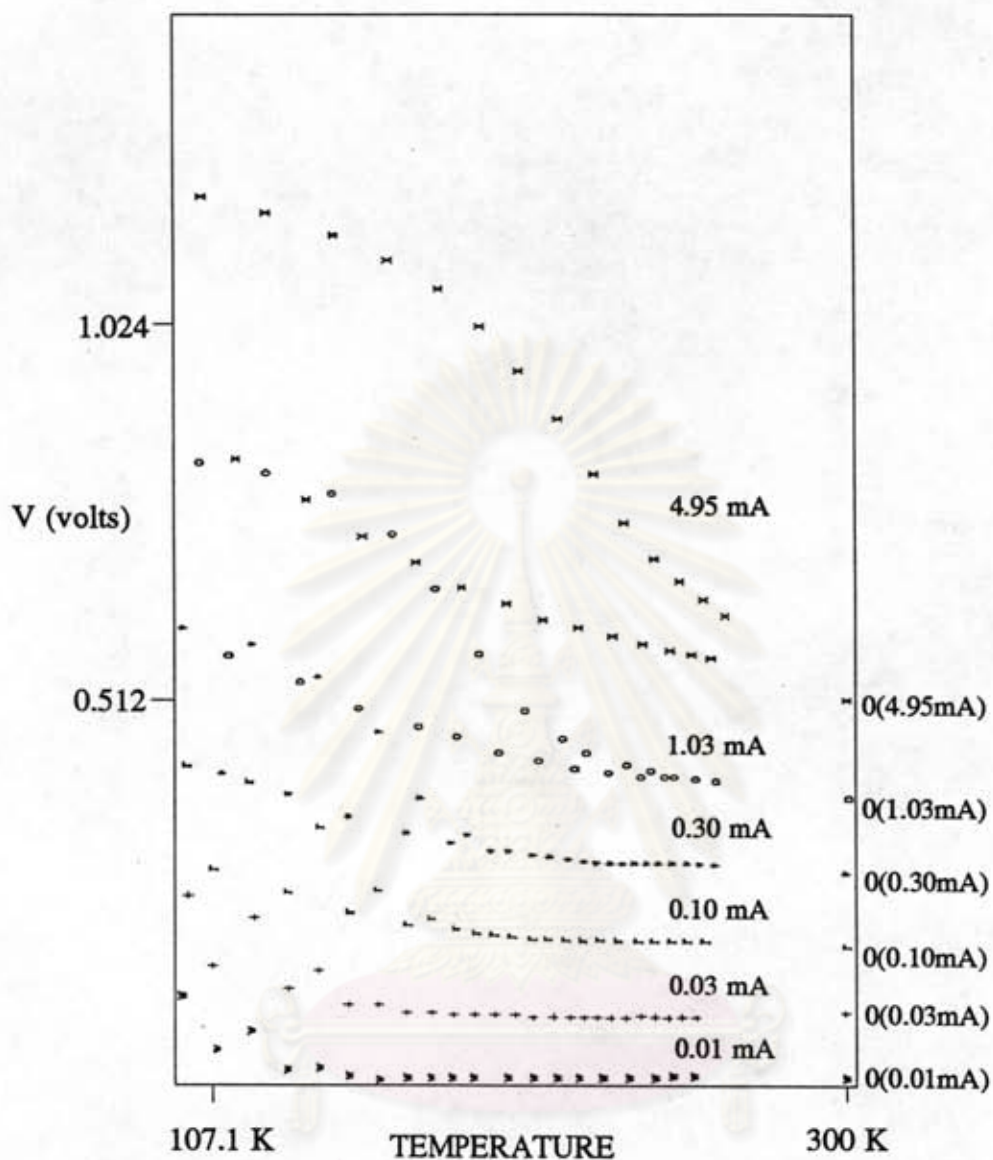


Fig.6 Sample of the data on the graph paper, #C3/25/2, Ni//p-CuInSe<sub>2</sub>. The x and y-axis are the thermocouple voltage (temperature) and the sample's absolute value of the voltage, respectively. The y-voltage includes voltage across the resistance used to shift the zero reference voltage of each constant current (see Appendix B), which shown at the temperature 300 K in this figure.



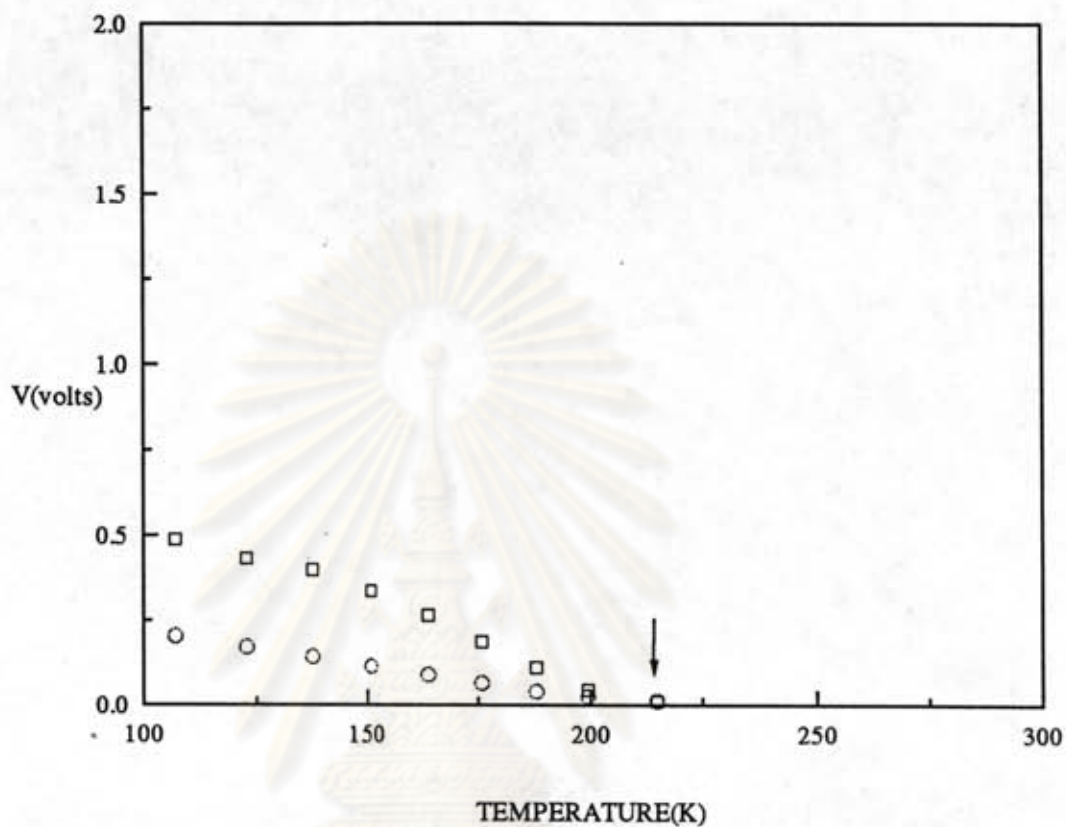


Fig.7a The graph of #C3/20, Au/p-CuInSe<sub>2</sub>, replotted at equal x-axis increments from graph paper like in Fig.6. The x-axis is now the temperature. The y-axis voltage absolute values on large area metal-semiconductor-small area metal at constant current now do not include the shifting voltage. The arrow is the split temperature  $T_s$ . The current is 0.01 mA.

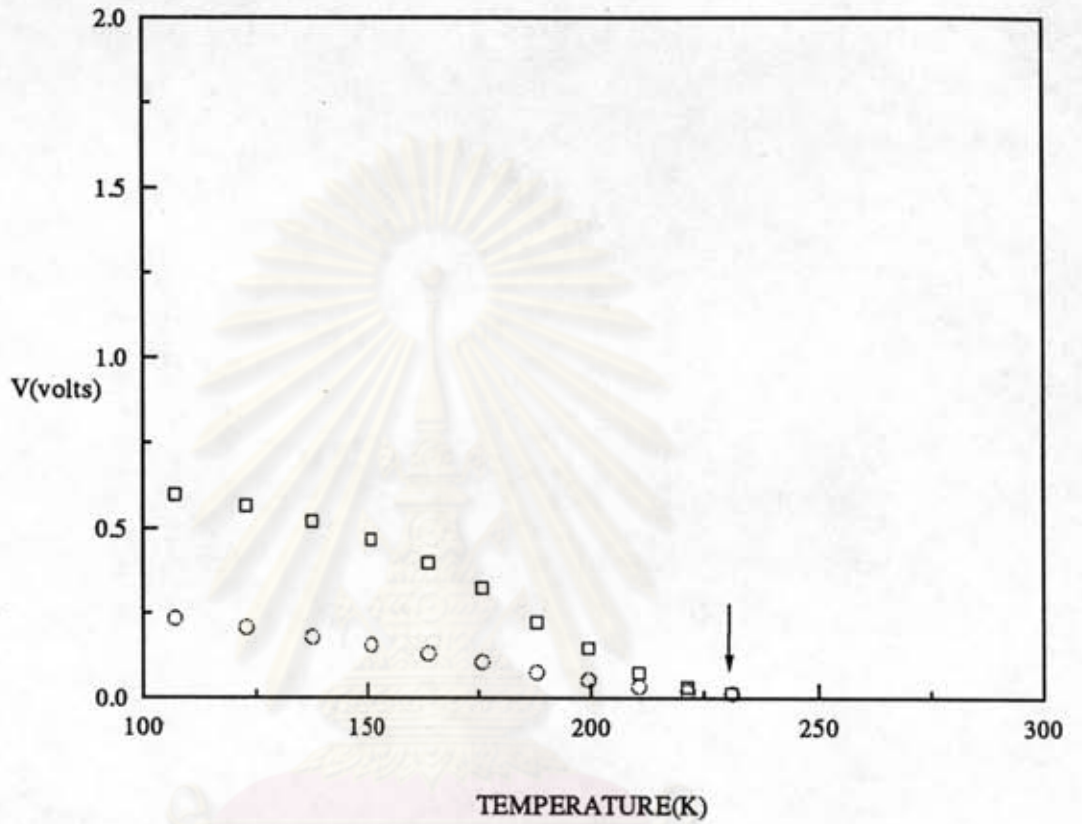


Fig.7b Replotted data of #C3/20 for constant current 0.03mA.

ศูนย์วิทยทรัพยากร  
จุฬาลงกรณ์มหาวิทยาลัย



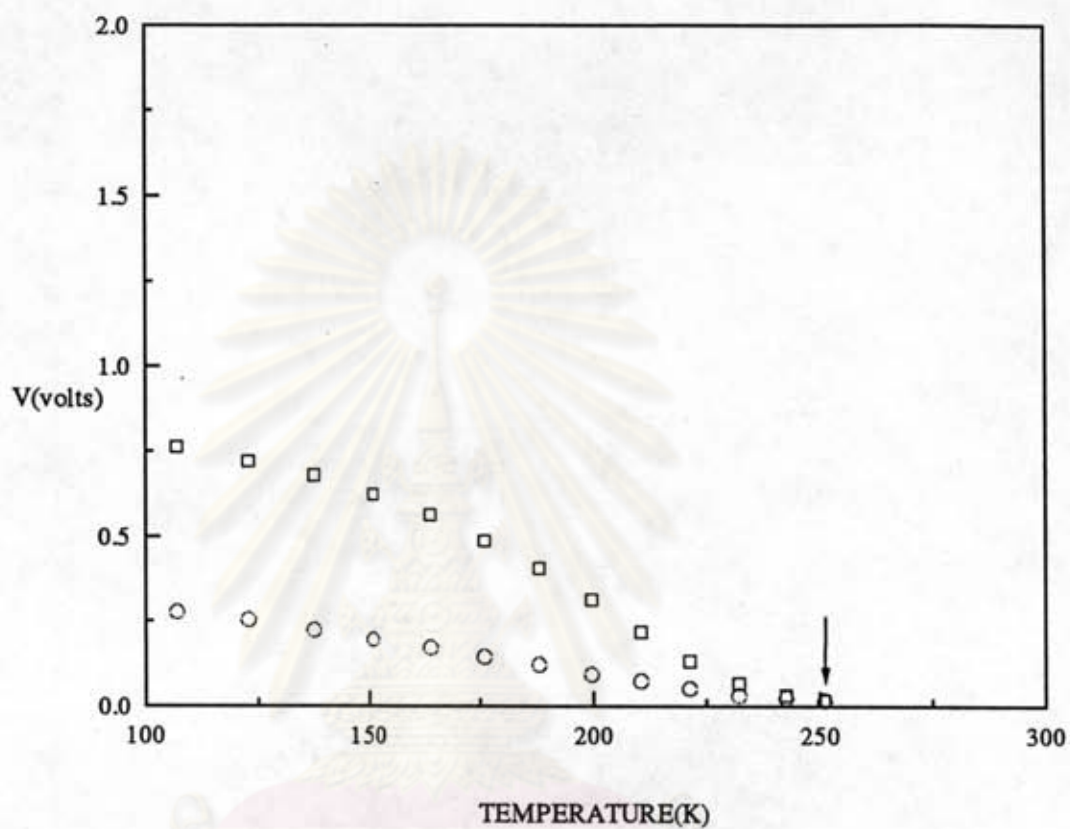


Fig.7c Replotted data of #C3/20 for constant current 0.1mA.

ศูนย์วิทยทรัพยากร  
จุฬาลงกรณ์มหาวิทยาลัย

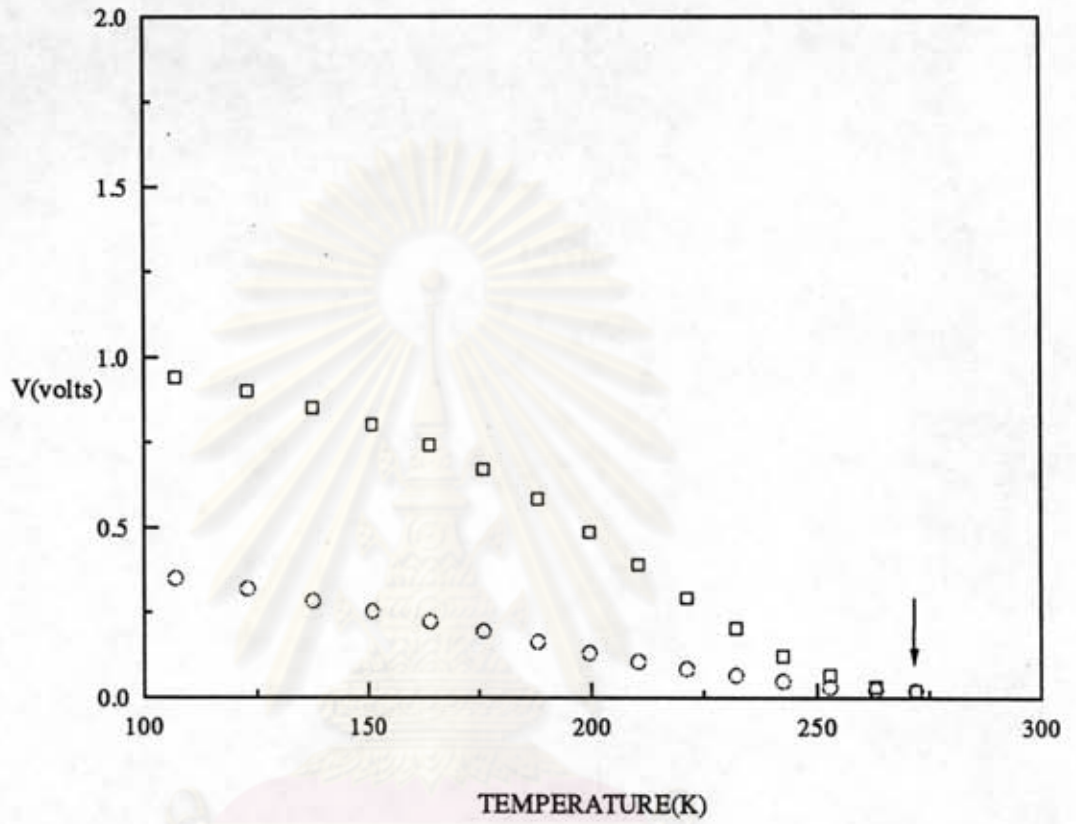


Fig.7d Replotted data of #C3/20 for constant current 0.3mA.

ศูนย์วิทยทรัพยากร  
จุฬาลงกรณ์มหาวิทยาลัย

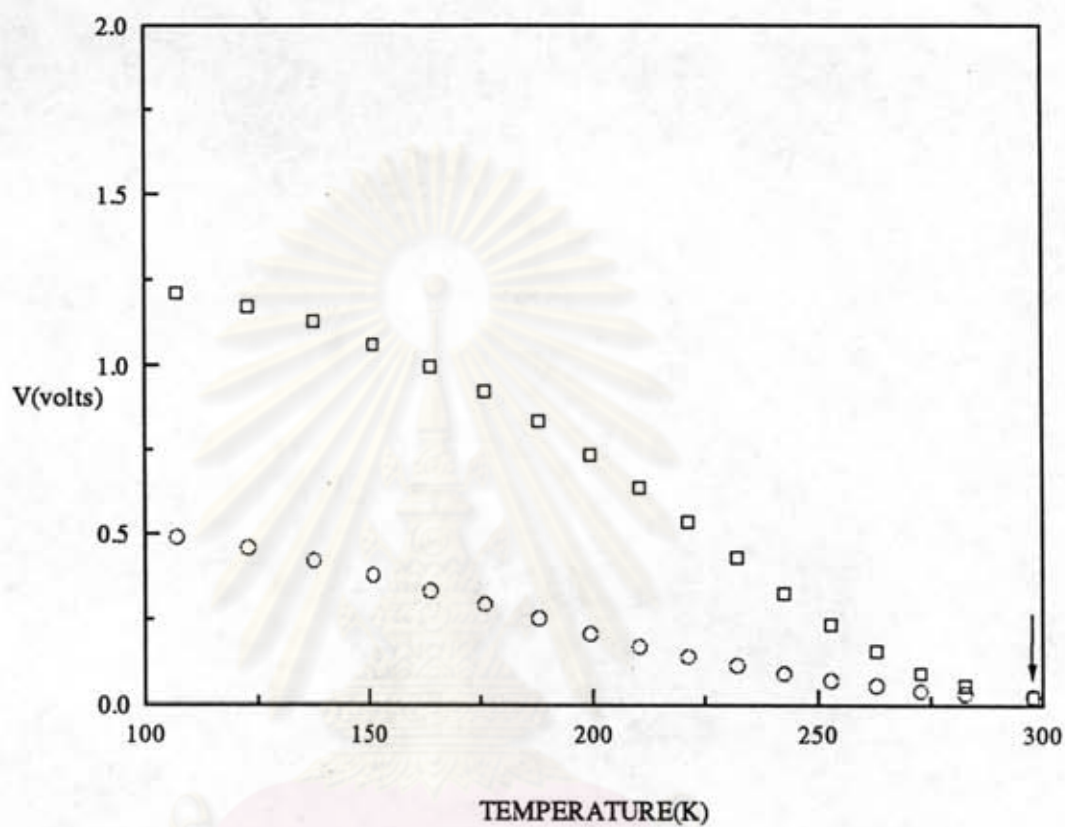


Fig.7e Replotted data of #C3/20 for constant current 1.03mA.

ศูนย์วิจัยทรัพยากร  
จุฬาลงกรณ์มหาวิทยาลัย



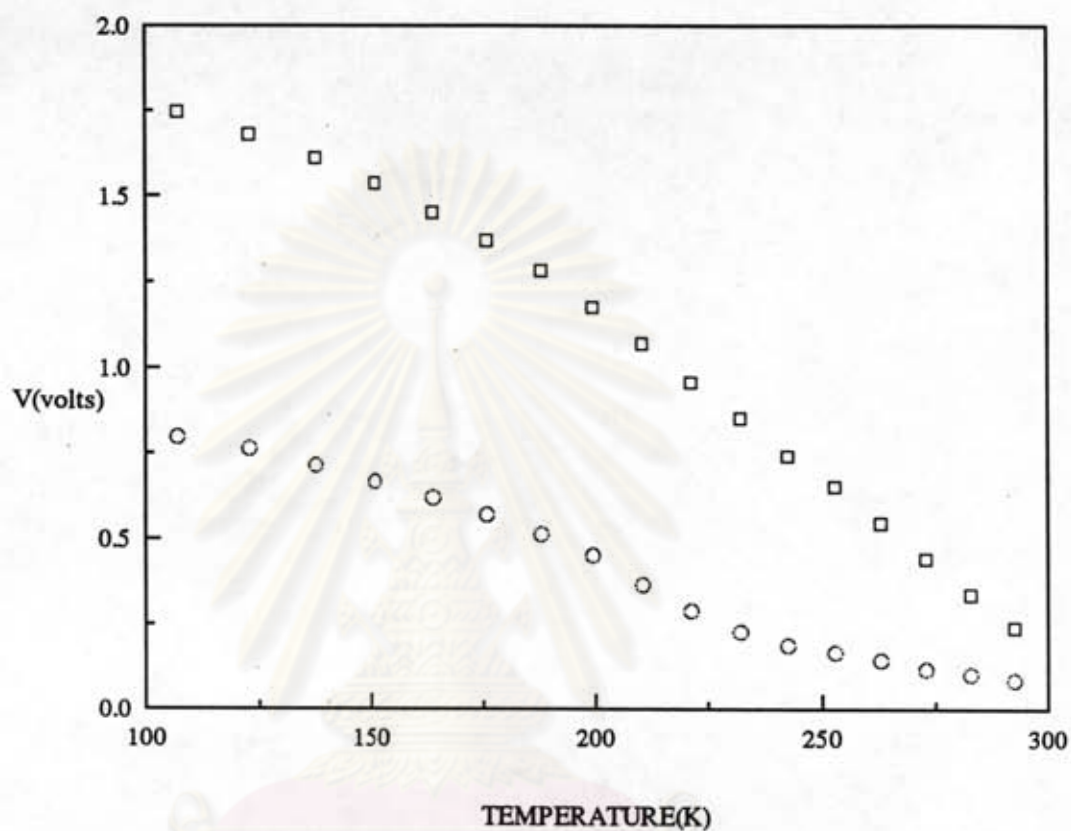


Fig 7f Replotted data of #C3/20 for constant current 4.95 mA.

ศูนย์วิทยาศาสตร์  
จุฬาลงกรณ์มหาวิทยาลัย

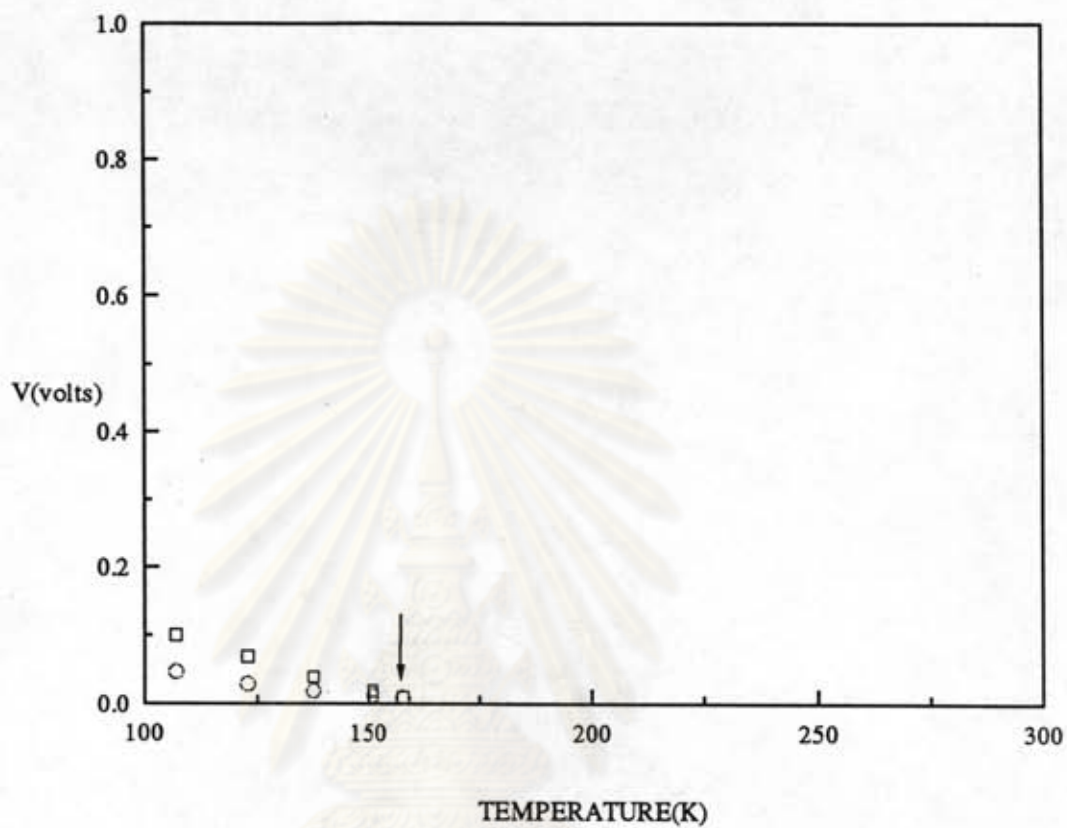


Fig.8a The graph of #C3/25/2, Ni/p-CuInSe<sub>2</sub>, replotted in the same way as in Figure 7. The current is 0.01 mA.

ศูนย์วิจัยทรัพยากร  
จุฬาลงกรณ์มหาวิทยาลัย

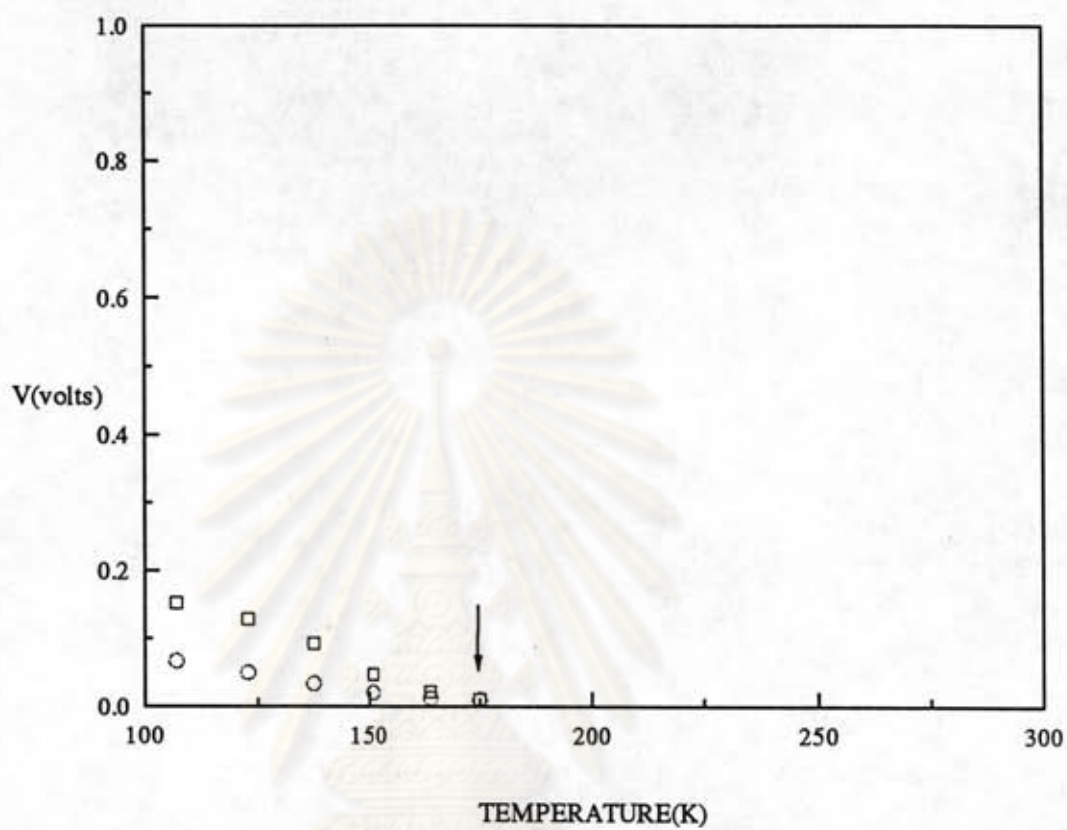


Fig.8b Replotted data of #C3/25/2 for constant current 0.03 mA.

ศูนย์วิทยทรัพยากร  
จุฬาลงกรณ์มหาวิทยาลัย



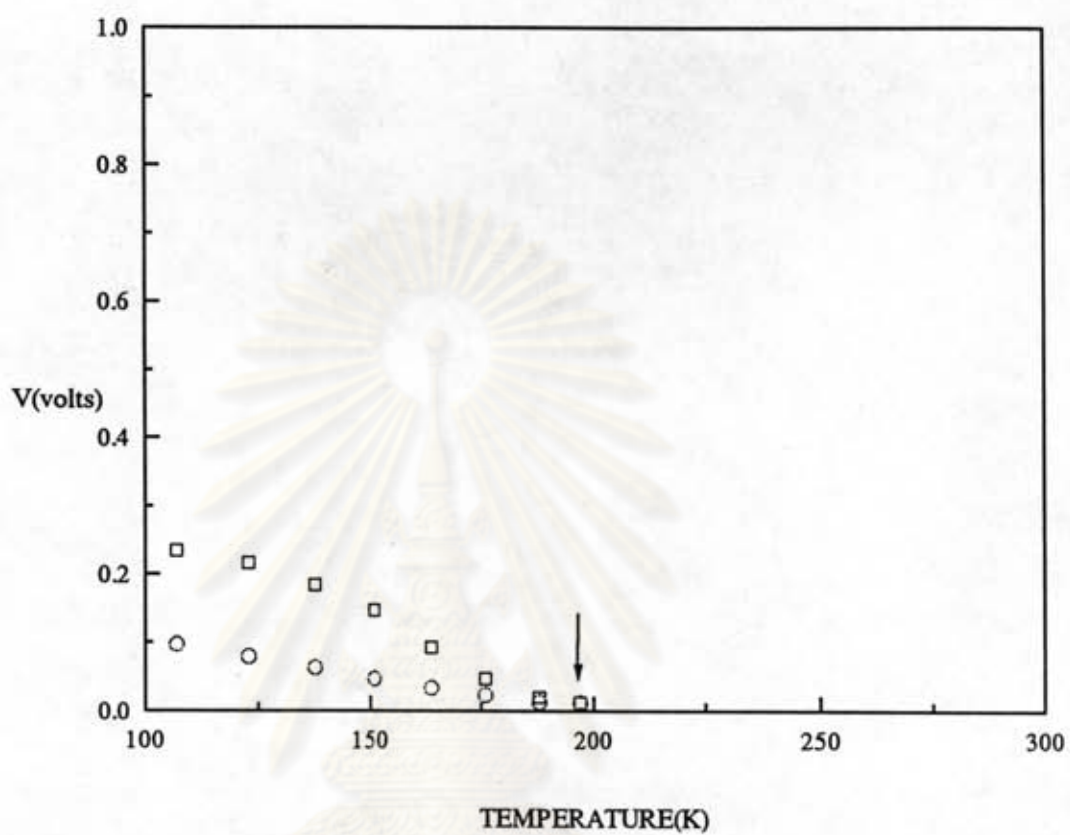


Fig.8c Replotted data of #C3/25/2 for constant current 0.1 mA.

ศูนย์วิทยทรัพยากร  
จุฬาลงกรณ์มหาวิทยาลัย

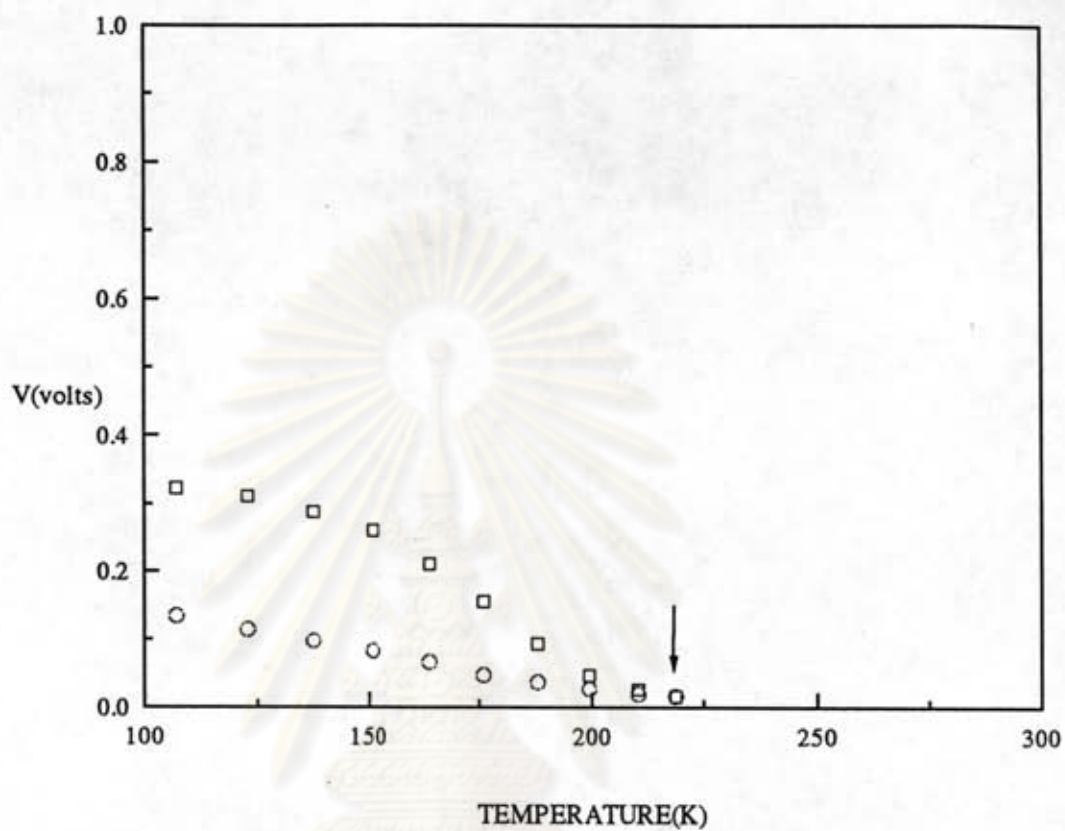


Fig.8d Replotted data of #C3/25/2 for constant current 0.3 mA.

ศูนย์วิทยทรัพยากร  
จุฬาลงกรณ์มหาวิทยาลัย

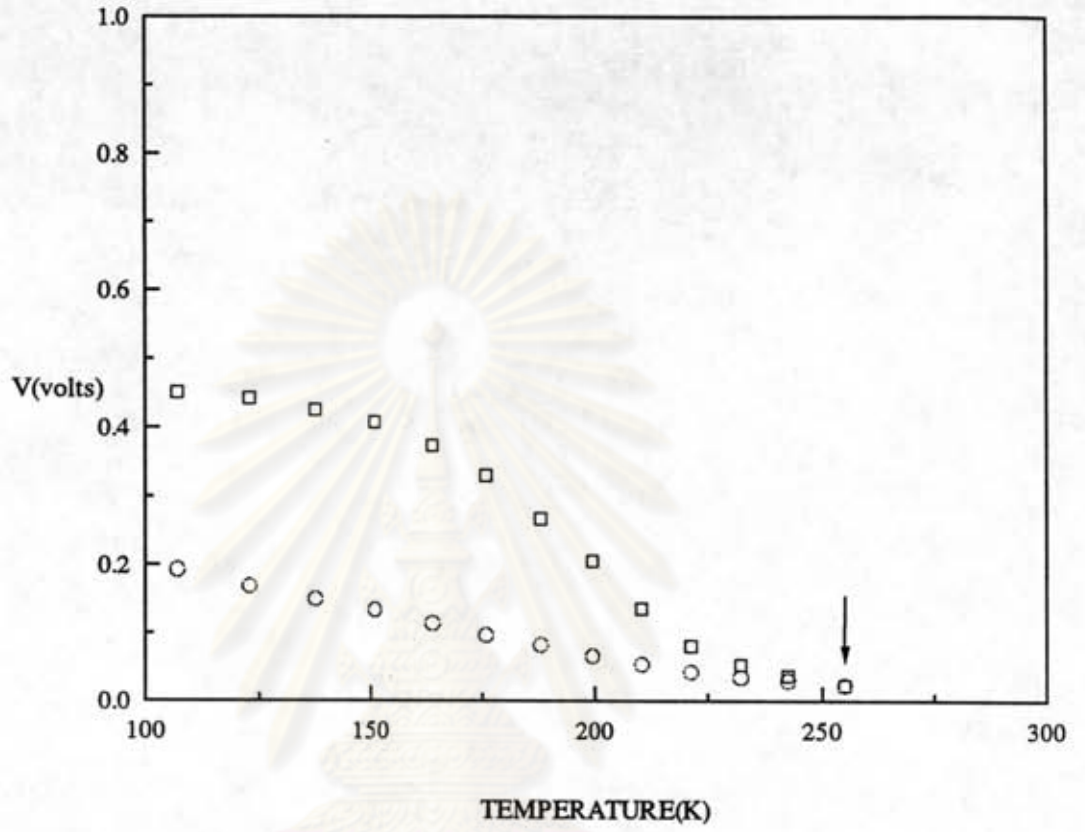


Fig.8e Replotted data of #C3/25/2 for constant current 1.03 mA.

ศูนย์วิทยาศาสตร์  
จุฬาลงกรณ์มหาวิทยาลัย



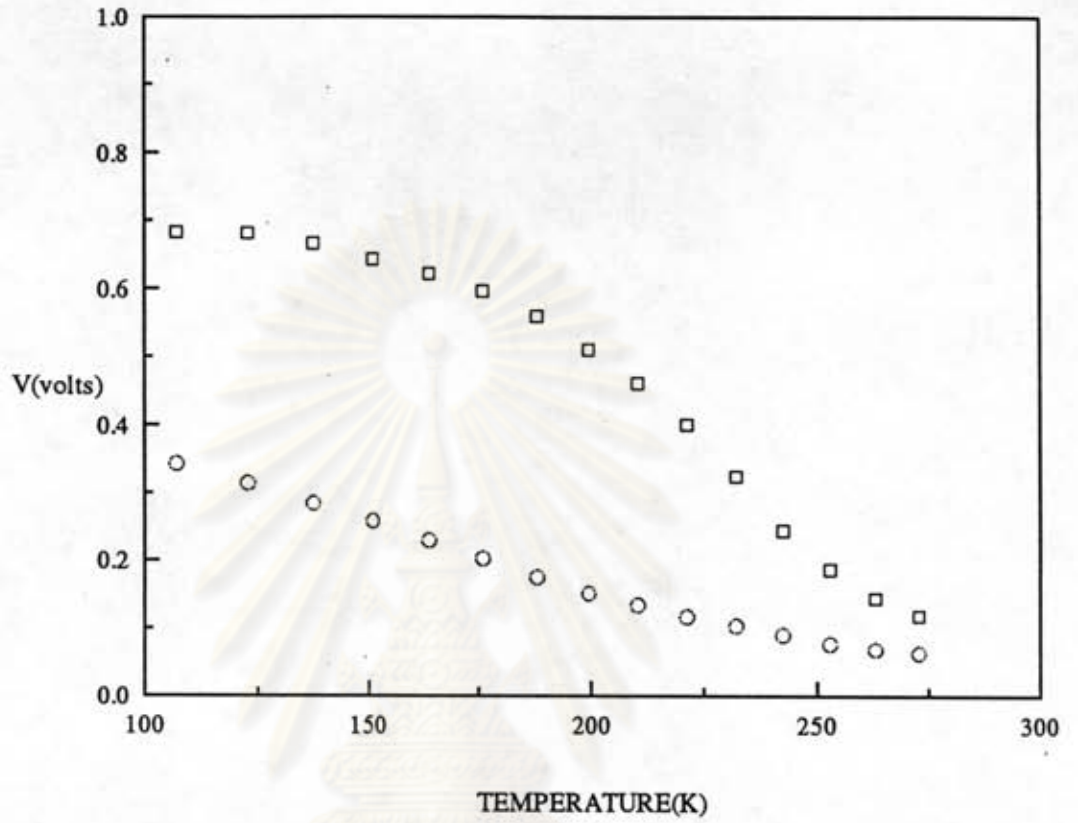
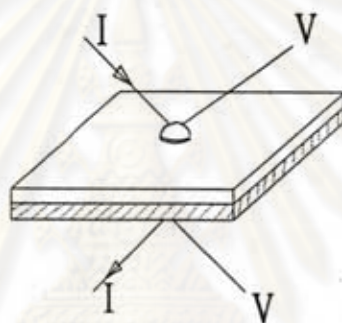


Fig.8f Replotted data of #C3/25/2 for constant current 4.95 mA.

ศูนย์วิทยทรัพยากร  
จุฬาลงกรณ์มหาวิทยาลัย

### 5.3 The Total Resistance and the Maximum Contact Resistivity of Au/p-CuInSe<sub>2</sub> and Ni/p-CuInSe<sub>2</sub>

I-V characteristics, at room temperature, between small area metal contact-semiconductor-large area metal contact, was measured by configuration in Fig.9. The typical I-V characteristics is shown in Fig.10. Total resistance  $R_t$  (i.e. resistance of the small area contact, the bulk, and large area contact) is determined from the slope.



**Fig.9** Schematic drawing of the total resistance measurement.

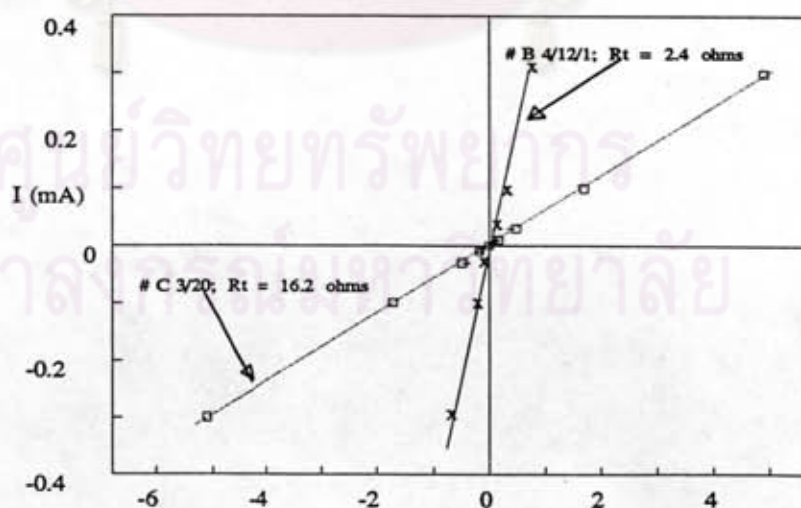


**Fig.10** I-V characteristics of #C3/20 and #B4/12/1, measured by the configuration in Fig.9.

The total resistance values are shown in Table 2. If the contact resistance of one electrode dominates, then  $R_t$  is the upperbound value of this contact resistance, defined here as  $\rho_c(\max)$ . Hence the values of the maximum contact resistivity  $\rho_c(\max)$ , i.e. small contact area multiplied by  $R_t$ , are also shown. The  $\rho_c(\max)$  value will be useful as the upper limit estimate of the contact resistivity determined by other measurement techniques.



ศูนย์วิทยทรัพยากร  
จุฬาลงกรณ์มหาวิทยาลัย

TABLE 2

Total resistance  $R_t$ , measured at room temperature.

#contact	contact area ( $\text{cm}^2$ )	$R_t$ ( $\Omega$ )	$\rho_c(\text{max})$ ( $\Omega\text{-cm}^2$ )
B3/5	$9.5 \times 10^{-3}$	93.0	0.88
B6/3/1	$9.5 \times 10^{-3}$	19.2	0.18
B6/3/2	$9.5 \times 10^{-3}$	23.6	0.22
B6/4	$9.5 \times 10^{-3}$	6.6	0.063
B4/9/1	$9.5 \times 10^{-3}$	6.3	0.060
B4/9/2	$9.5 \times 10^{-3}$	4.2	0.040
B4/11/1	$4.4 \times 10^{-3}$	5.2	0.023
B4/11/2	$9.5 \times 10^{-3}$	2.7	0.026
B4/11/3	$2.8 \times 10^{-2}$	1.1	0.031
B4/11/4	$5.7 \times 10^{-2}$	1.8	0.10
B4/11/5	$4.4 \times 10^{-3}$	11.0	0.048
B4/12/1	$9.5 \times 10^{-3}$	2.4	0.023
B4/12/2	$9.5 \times 10^{-3}$	3.6	0.034
C3/16	$9.5 \times 10^{-3}$	9.3	0.088
C3/20	$9.5 \times 10^{-3}$	16.2	0.154
D3/4	$9.5 \times 10^{-3}$	18.9	0.180
B4/17/1	$9.5 \times 10^{-3}$	13.2	0.125
B4/17/2	$9.5 \times 10^{-3}$	5.3	0.050
B6/1/1	$9.5 \times 10^{-3}$	7.4	0.070
B6/1/2	$9.5 \times 10^{-3}$	9.1	0.087
C3/15/1	$9.5 \times 10^{-3}$	13.6	0.129
C3/15/2	$9.5 \times 10^{-3}$	11.8	0.112
C3/25/1	$9.5 \times 10^{-3}$	13.2	0.125
C3/25/2	$9.5 \times 10^{-3}$	4.0	0.038
D3/3	$9.5 \times 10^{-3}$	13.3	0.126



Here, contacts which the labels differ only the last label were on the same substrate. For example #B4/17/1 and #B4/17/2 were on the same substrate, i.e. #B4/17 in Table1.

#### 5.4 Contact Resistivity of Mo/p-CuInSe<sub>2</sub>

I-V characteristics, at room temperature, between Mo-semiconductor-Mo, with equal area contacts on the same surface of as-deposited (AD) and after successive heat treatment at 250 °C (10 min in H<sub>2</sub>), are shown in Fig.11.

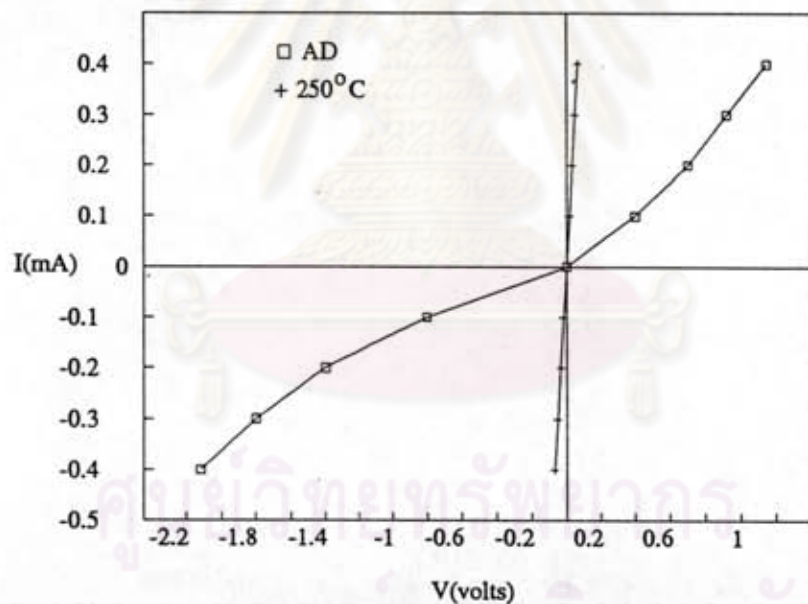


**Fig.11** Typical I-V characteristics of Mo/p-CuInSe<sub>2</sub>, as-deposited (AD) and after 250 °C heat treatments.

For a crude value of contact resistivity, the total resistance is assumed to be the resistance of two identical Mo contacts, the resistance in the bulk is neglected. The contact resistivity was calculated, by divided the total resistance by 2 and then multiply by the contact area, at 0.4 mA which is the current

density that close to the maximum current density of solar cells, i.e. 40 mA/cm<sup>2</sup>. It is upper bound value of contact resistivity of Mo/p-CuInSe<sub>2</sub>. The results are summarized in Table 3. Also shown are the values after subsequent heat treatment at 450 °C (10 min in H<sub>2</sub> ).

**TABLE 3**

Upper bound value of contact resistivity of Mo/p-CuInSe<sub>2</sub>.

All contacts have contact area  $7.9 \times 10^{-3}$  cm<sup>2</sup>.

#Substrate	between contacts	$\rho_c$ (AD) ( $\Omega$ -cm <sup>2</sup> )	$\rho_c$ (250 °C) ( $\Omega$ -cm <sup>2</sup> )	$\rho_c$ (450 °C) ( $\Omega$ -cm <sup>2</sup> )
B4/18	1 - 4	20.3	2.7	< 1.1*
B4/18	2 - 5	13.0	4.1	< 0.2*
C3/26	1 - 2	21.0	8.4	< 0.2*
C3/27	1 - 4	15.8	0.8	nd.
C3/27	2 - 5	11.4	0.6	< 0.7*
C3/27	3 - 6	20.8	0.5	< 0.1*

where \* in the last column indicates that after the heat treatment the Mo film itself became appreciably more resistive with an ohm-meter reading of the order of  $10^1 \Omega$  across the same dot. So, the true contact resistivity at 450 °C heat treatment should be appreciably less than the values in the last column. If low contact resistance resulted from the 450 °C heat treatment, this configuration ,i.e.

using two probes on the same surface yields large error. Another measurement configuration is needed. Nevertheless, it does show the trend of decrease contact resistivity with increase heat treatment.

### 5.5 Contact Resistivity by Approximate Measurement

In order to measure the contact resistance (resistivity) of a circular dot, the configuration in Fig.12 is used. This configuration employs four probes arranged slightly differently from that of Toro configuration which employs three probes. However, both configurations are based on the same principle, i.e. to measure the approximate contact resistance of interest directly under one-dimensional current flux while other resistance are excluded.

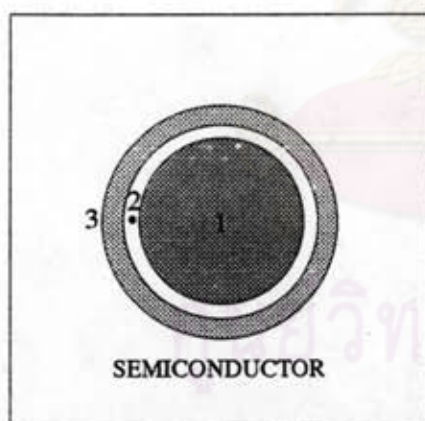


Fig.12A Top view.

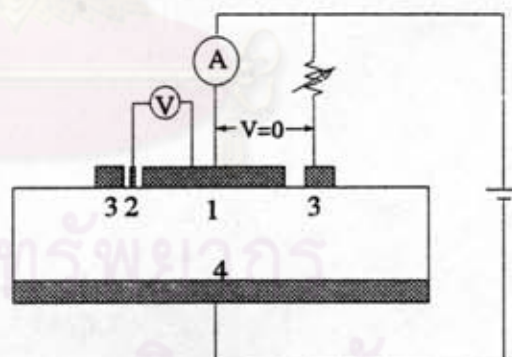
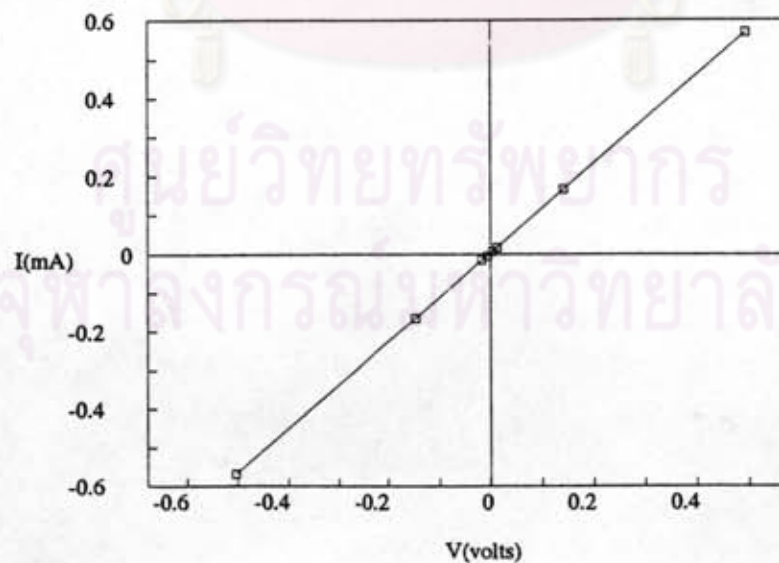


Fig.12B Side view.

**Fig.12** Four probes configuration used in measuring the contact resistance of contact 1 by excluding the spreading conductance. Note the current between 1 and 4 can be forced to be only vertical.



In the measurement, the adjustable resistance in Fig.12, which was used to compensate the resistance of ammeter, was adjusted until there is no current between probes 1 and 3, i.e.  $V_{13} = 0$ . So,  $V_{12}$  is including the voltage drop between contact 1 (interested contact) and an equipotential surface extended from the high resistive layer just beneath this contact on to the surface. Graph between  $I_1$  and  $V_{12}$  is shown in Fig.13, and contact resistance  $R_{\text{approx}}$  was determined from the slope. Because the equipotential surface's curvature is undetermined, its position indicated by  $V_{12}$  is only "somewhere below" contact 1. This resistance value is therefore good for approximate determination of the contact resistance. Note also that the equipotential surface "spacing" per  $\Delta V$  can be different in the depth direction;  $V(\text{depth})$  is not necessarily linear as for example in the depletion region. While it is only an approximate measurement, the latter does infer a major fraction of the resistance of interest and in this thesis we beg to use the term  $R_{\text{approx}}$  for the "contact resistance" measured in this way.



**Fig.13** Typical I-V characteristics between  $I_1$  and  $V_{12}$ . The contact resistance of contact 1 is calculated from the slope.



Results of the measurement are summarized in Table 4. Also shown are contact resistivity  $\rho_c(\text{approx})$  which obtained from  $R_{\text{approx}}$  multiplied by the contact area. Also shown for comparison are  $R_t$  and  $(R_{\text{approx}} / R_t)$ .

**TABLE 4**

Contact resistance and contact resistivity of Au/p-CuInSe<sub>2</sub>  
measured by approximate method.

#contact	$R_{\text{approx}}$	$R_t$ ( $\Omega$ )	$\rho_c(\text{approx})$ ( $\Omega\text{-cm}^2$ )	$R_{\text{approx}} / R_t$ (%)
# C3/20	9.2	16.2	0.087	55
# B4/11/3	0.84	1.1	0.024	76
# B4/nd/2	2.1	2.54	0.020	83

where #B4/nd/2 , the substrate which is not in Table1.